

UIIU-ENG 86-3602

Report No. 125

PREDICTING THE FATIGUE LIFE OF WELDS
UNDER COMBINED BENDING AND TORSION

by

J.-Y. Yung and F. V. Lawrence, Jr.
Departments of Civil Engineering and Metallurgy

A Report of the
MATERIALS ENGINEERING - MECHANICAL BEHAVIOR
College of Engineering, University of Illinois at Urbana-Champaign
April 1986

PREDICTING THE FATIGUE LIFE OF WELDS
UNDER COMBINED BENDING AND TORSION

J.-Y. YUNG and F.V. LAWRENCE, JR.

Departments of Civil Engineering and Metallurgy, University of Illinois
at Urbana-Champaign, Urbana, IL 61801, U.S.A.

Abstract-- Tube-to-plate weldments were fatigue tested under combined bending and torsion loadings. The initiation and early growth of cracks were restricted to the weld toe. Compressive residual stresses were measured at the weld toe using X-ray methods. Thermal stress relief lowered the weld-toe residual stresses and reduced the fatigue life. Two approaches were investigated to predict the fatigue crack initiation life.

The first approach used three different strain-based parameters: the maximum shearing strain amplitude, the Lohr-Ellison parameter and the Kandil-Brown-Miller parameter. These parameters were combined with the Coffin-Manson equation to predict the fatigue crack initiation life under multiaxial cyclic stresses. The required notch-root strains were calculated using an elastic-plastic finite element analysis.

In a second approach, the Basquin equation was modified to estimate the fatigue life of welds for lives greater than 10^5 cycles. The worst-case-notch condition was assumed to be valid for both torsion and bending. The predicted fatigue lives were within a factor of three of the observed fatigue lives of the tube-to-plate weldments.

LIST OF SYMBOLS

- b = Fatigue strength exponent
- c = Fatigue ductility exponent
- E = Modulus of elasticity
- k, s = Constants
- K_{fmax} = Maximum fatigue notch factor
- N_I = Cycles to crack initiation and early growth
- N_f = Cycles to failure
- S_a = Nominal stress amplitude
- γ = Shear strain
- γ^* = Maximum shear strain on plane intersecting the free surface at 45 deg.
- γ_{max} = Maximum shear strain
- ϵ_f' = Fatigue ductility coefficient
- ϵ_n = Strain normal to γ_{max} plane
- ϵ_n^* = Strain normal to γ^* plane
- ϵ = Normal strain
- τ_a = Shear stress amplitude
- σ_a = Local stress amplitude
- σ_f' = Fatigue strength coefficient
- σ_{no} = Mean stress normal to γ_{max} plane
- σ_{no}^* = Mean stress normal to γ^* plane
- σ_r = Residual stress

Superscripts

B = Bending

E = Equivalent stress

P = Principal stress

T = Torsion

THE APPLICATION OF MULTIAXIAL FATIGUE CONCEPTS TO WELDMENTS

Weldments are often subjected to multiaxial loading as are many notched, structural components: welded girders and shafts are common examples. Weldments differ from other notched structural components in at least two respects: welding usually induces high residual stresses at the fatigue crack initiation sites; and welds are irregular and therefore difficult notches to quantify.

Weld toes are frequently the sites of fatigue crack initiation and can be regarded as two dimensional notches of infinite length. While the stresses and strains normal to the weld are greatly magnified at the weld-toe notch root and lead to fatigue failure, there is mounting evidence that stresses and strains parallel to the line of the notch root may also increase the severity of the problem despite the fact that stresses and strains parallel to the toe have rather low concentration factors. Previous studies of Munse [1] suggested that shearing stresses reduce the fatigue life of weldments and that better correlations between fatigue life test data and applied stress can be obtained using the principal stresses near the weld toe rather than the stresses and strains normal to the toe.

The object of this study was to apply recent ideas in multiaxial fatigue theory to tube-to-plate weldments subjected to bending and torsion

loading. Most multiaxial fatigue theories attempt to predict multiaxial fatigue behavior using uniaxial fatigue data. Early studies correlated multiaxial fatigue data with the maxima of principal strain amplitude, shear strain amplitude, or octahedral strain amplitude. Recent work emphasizes the concept of a critical plane for crack initiation and growth. Lohr and Ellison [2] proposed the following relationship based on the maximum shear strain on planes intersecting the free surface and the strain normal to the crack plane:

$$\gamma^* + k\epsilon_n^* = \text{constant} \quad (1)$$

where γ^* = the maximum shear strain amplitude on planes intersecting the free surface at 45 degrees which drives the crack through the thickness.
 ϵ_n^* = the strain amplitude normal to the γ^* plane.
 k = constant, 0.4 for 3 steels.

Kandil, Brown and Miller [3] proposed a similar relationship based on the maximum shear strain amplitude and the strain normal to the crack plane:

$$\frac{\Delta\gamma_{\max}}{2} + s\epsilon_n = \text{constant} \quad (2)$$

where $\Delta\gamma_{\max}/2$ = the maximum shear strain amplitude
 ϵ_n = the strain amplitude normal to the plane
 s = 1 when strain amplitude is used in the expression.

While neither of the above relationships includes the effects of mean stress, the influence of the mean stress normal to the shear plane (σ_{no}) can be incorporated by modifying the shear strain parameters [4,5]. Fash and Socie [4,5] combined several of the above mentioned parameters and relationships with the well known Coffin-Manson equation which describes strain controlled fatigue and obtained the following expressions:

$$\frac{\Delta \gamma_{max}}{2} = 1.3 \frac{\sigma_f'}{E} (2N_f)^b + 1.5 \epsilon_f' (2N_f)^c \quad (3)$$

$$\gamma^* + 0.4 \epsilon_n^* + \frac{\sigma_{no}^*}{E} = 1.44 \frac{\sigma_f'}{E} (2N_f)^b + 1.60 \epsilon_f' (2N_f)^c \quad (4)$$

$$\frac{\Delta \gamma_{max}}{2} + \epsilon_n + \frac{\sigma_{no}}{E} = 1.65 \frac{\sigma_f'}{E} (2N_f)^b + 1.75 \epsilon_f' (2N_f)^c \quad (5)$$

The fatigue crack initiation life of the 20 tube-to-plate weldments investigated were compared with fatigue crack initiation life estimates made using the three relationships above and an analysis based on the Basquin equation and the fatigue notch factor concept. While estimates of the fatigue crack propagation life could have in principle been obtained using the concept of the effective stress intensity factor, no such estimates were made in this study because of the complex nature of fatigue crack growth and the lack of a model for the stress intensity factor for the geometry of the test pieces used in this study.

EXPERIMENTAL METHODS AND RESULTS

Tube-to-plate weldments having the geometry and dimensions shown in Fig. 1 were fabricated from seamless, cold-drawn steel tubing meeting the ASTM A519 standard and having a yield strength of 552 MPa and an ultimate strength of 700 MPa. Welding was carried out using an automatic gas-metal-arc process operated at 25 volts and 150 amperes with an argon 2% oxygen shielding gas. The solid, filler-metal wire had a diameter of 0.89 mm and met the AWS E70S standard. The weld size was approximately equal to the tube thickness. Both as-welded and stress-relieved (650°C for 4 hours) test pieces were prepared. Stress relief did not greatly alter the hardness of the weld-region microstructures as is shown in Fig. 2.

The axial and circumferential residual stresses which developed during welding were measured using X-ray diffraction methods. Residual stresses were measured at weld toe and along a path away from the toe and down the axis of the tube. The variation of residual stresses on the interior of the tube were measured by successively electropolishing material from the outer surface. The measured and calculated residual stresses are listed in Table 1. Figure 3 shows the variation of residual stress at the surface of the tube. The results of the residual stress measurements confirm that girth welds can have compressive residuals at their weld toes [6].

The test apparatus used was designed for the bi-axial fatigue program of the Society of Automotive Engineers Fatigue Design and Evaluation Committee [4]. As can be seen in Fig. 4, specimens were clamped into the load yoke and the test frame. Any combination of bending and torsion could be applied by adjusting the amplitude and phase of the two independent, hydraulic actuators. Tests on the tube-to-plate weldments were carried out under load control using completely-reversed, constant-amplitude bending, combined

bending and torsion, and pure torsion load cycles. The fatigue test results are listed in Table 2 and plotted in Figs. 6-8. The fatigue test data are plotted in the S-N diagrams of Figs. 6-8 using several definitions of stress: bending stress (neglecting any torsional stresses), equivalent stress (von Miseses criterion) and maximum principal stress. The test data correlate best when plotted against the maximum principal stress which includes the effect of the torsional shearing stresses. Shearing stresses reduced the fatigue life of tube-to-plate welds subjected to combined bending and torsion as had been observed earlier by Munse [1]. All specimens failed at the weld toe on the tube. The fracture surfaces of the welds subjected to combined bending and torsion had a characteristic "factory-roof" appearance.

Crack initiation was monitored using the pulse-echo ultrasonic technique with surface wave transducers, but this method did not give reliable indications of small initiated fatigue cracks. Replicas of the weld toe were taken periodically to establish the presence of an initiated crack. The replica studies indicated that multiple crack initiation occurred at the weld toe and that initiation and early growth were constrained to the line of the weld toe as had been the experience of Fash [7] with notched shafts. Two stress-relieved specimens were removed from the testing apparatus and heat-tinted at lives corresponding to calculated estimates of the fatigue crack initiation lives (N_I).

FINITE ELEMENT STUDIES

The relationships between the remote and the notch-root stresses and strains were studied using elastic-plastic finite element methods. The ABAQUS [8] software with three-dimensional, twenty-noded solid elements was

used to generate the mesh shown in Fig. 5. A notch-root radius of 0.25 mm was established at the weld toe which value corresponds to the worst-case, notch-root condition [9]. The stabilized cyclic notch-root material properties used in the finite element calculations were estimated based on hardness measurements and metallography of the weld microstructural zones and on previous studies of the fatigue properties of ASTM A36 weld microstructures [10]. The elastic stress concentration factors for bending and torsion were found to be 4.06 and 1.90, respectively.

The ABAQUS software has provisions for considering the effects of residual (initial) stresses; however, our experience was that this initial stress condition subroutine would work for tensile but not compressive residual stresses. Consequently, Table 3 lists calculated results only for the stress-relieved test pieces.

ESTIMATES OF THE FATIGUE CRACK INITIATION LIFE USING MULTIAXIAL THEORIES

The analytical estimates of the fatigue crack initiation lives listed in Table 4 were obtained using Eqs. 3-5 and notch root strains predicted from the remote loading conditions and the results of the FEM analysis summarized in Table 3. The most reliable measurements of initiated crack size were provided by two heat-treated specimens which were heat-tinted at lives corresponding to calculated values of fatigue crack initiation life. These test pieces were subjected to combined bending and torsion ($\tau_a^T/S_a^B = 0.58$). Although battering of the fracture surfaces by the reversed loadings nearly eradicated the distinction between the heat-tinted fractured and the other fractured regions in the two specimens, crack depths of 1.2 mm and 1.4 mm could be measured at lives of 1,538 and 77,000 cycles. These lives corresponded to the crack initiation lives (N_I) predicted by the

Kandil-Brown-Miller parameter and the Coffin-Manson relationship (see Eq. 5 and Table 4) and accounted for 4% and 50% of the observed total fatigue lives ($N_f \approx 39,000$ and 150,000 cycles), respectively. These results are in accord with our general belief (based on experience with other welds subjected to uniaxial cyclic stresses) that crack initiation and early growth become increasingly important and, indeed, dominant at long lives.

ANALYTICAL ESTIMATES OF THE TOTAL FATIGUE LIFE USING THE BASQUIN EQUATION

If at long lives fatigue crack initiation becomes dominant, then estimates of the crack initiation life can be used as approximations to the total fatigue life. The authors have been using the Basquin equation to estimate the fatigue resistance of welds subjected to axial and bending stresses at lives greater than 10^6 cycles [11]. This approach assumes worst-case-notch conditions for the value of the fatigue notch factor K_f . These concepts were applied to the tube-to-plate welds of this study as an alternate approach to predicting their total fatigue lives. We assumed that the worst-case-notch idea was also valid for welds subjected to torsion and that at long lives the local stress-strain behavior was elastic. The local equivalent stress amplitude predicted by the von Mises criterion (σ_a^E) and the maximum principal stress amplitude (σ_a^P) are given by the expressions below:

$$\sigma_a^E = [(K_{fmax}^B S_a^B)^2 + 3(K_{fmax}^T \tau_a^T)^2]^{1/2} \quad (6)$$

$$\sigma_a^P = (K_{fmax}^B S_a^B / 2) + [(K_{fmax}^B S_a^B / 2)^2 + (K_{fmax}^T \tau_a^T)^2]^{1/2} \quad (7)$$

where the superscripts B and T indicate bending and torsion, respectively. For completely reversed loading, the local mean stress will be equal to the residual stress at the weld toe. While Niku-Lari [12] used both Dang Van's criterion and the von Mises criterion to estimate the combined effects of mean and residual stresses in unnotched specimens, it seems most reasonable for notched specimens such as the welds considered here to use the component of residual (and mean) stress perpendicular to the weld toe inasmuch as the initiation and early growth of fatigue cracks was confined to the line of the weld toe. The modified Basquin equation becomes:

$$\sigma_a^E \text{ (or } \sigma_a^P) = (\sigma_f' - \sigma_r)(2N_f)^b \quad (8)$$

From the elastic-plastic finite element analyses for the worst-case-notch condition (notch root radius equal to Peterson's parameter a), the elastic stress concentration factors for bending and torsion were found to be 4.06 and 1.90, respectively. The corresponding values of the worst-case fatigue notch factor (K_{fmax}) were 2.53 for bending and 1.45 for torsion. The average longitudinal residual stress at a 0.25 mm depth was -431 MPa for the as-welded condition. Ten percent of this residual stress was assumed to persist after the stress relief treatment [13]. The fatigue properties of the HAZ were estimated using measured hardness values and empirical relationships in [14]. Total life estimates made using the Basquin equation and the approach outlined above are given in Table 5. Comparisons of the fatigue lives predicted using the Basquin equation approach (Eq. 8) and the observed lives are plotted in Figs. 9-11. The predictions agree with the observed lives within a factor of three except for the comparison based on bending stresses only (Fig. 9).

observed lives within a factor of three except for the comparison based on bending stresses only (Fig. 9).

SUMMARY AND CONCLUSIONS

Although a limited number of tests were performed in this short study, several conclusions can be drawn: The tube-to-plate welds proved to be a successful geometry for the study of the combined effects of bending and torsion on weldments. The combined bending and torsion loadings studied gave lives about a factor of three shorter than pure bending stresses, so that multi-axial stress states do influence the fatigue resistance of weldments despite the two-dimensional nature of the weld-toe notch and its relative insensitivity to pure torsional loading. Residual stresses were found to play an important role in determining the fatigue life period devoted to crack initiation and early growth. The multi-axial fatigue theories of Lohr and Ellison and Kandil, Brown and Miller both gave reasonable estimates of fatigue crack initiation life when the notch root strains could be determined. For applications involving notches, one must resort to methods such as elastic-plastic finite element analyses to estimate the required notch-root strains. Estimates of initiation life based on Basquin's equation modified for multi-axial stresses gave predictions for long-life fatigue life which were within a factor of three of the observed total lives.

ACKNOWLEDGEMENTS

This study was supported by the University of Illinois Fracture Control Program which is funded by a consortium of midwest ground vehicle industries. The authors wish to thank Professor Darrel Socie of the Department

of Mechanical Engineering and Dr. James W. Fash for the use of their test apparatus and their kind assistance in setting up the experiments described.

Table 1

Residual stress distribution for as-welded tube-to-plate specimens

Location Distance from Weld Toe, mm.	Depth mm.	Measured and Calculated Residual Stress, MPa		
		Longitudinal*	Tangential*	Radial**
weld toe	0.	-534	42	0
	0.05	-430	-82	0
	0.13	-272	29	0
	0.25	-328	-102	0
	0.51	-367	79	0
	1.00	-283	36	-1
38	0.	-366	-279	0
	0.05	-189	4	0
	0.13	-188	-81	0
	0.25	-185	-144	1
	0.51	-318	-108	2
	1.00	-271	-87	4
76	0.	-311	-356	0
	0.05	-236	-56	0
	0.13	-198	-86	0
	0.25	-278	-134	1
	0.51	-347	-29	2
	1.00	-229	-157	4
114	0.	-267	-97	0
	0.05	-197	-39	0
	0.13	-188	-138	0
	0.25	-132	-146	1
	0.51	-108	-44	2
	1.00	-118	-33	3

* : measured values

** : calculated values

Table 2

Fatigue test results for tube-to-plate welds

Welds	Weld Toe Bending Moment	Torsion N-m	Fatigue Life N_f , cycles
as-welded	974	-	76,660
	925	-	198,000
	852	-	145,690
	733	-	560,850
	674	-	624,330
	974	677	27,100
	925	1057	47,090
	925	704	78,620
	733	847	93,690
	674	779	220,030
	550	637	788,370
	550	637	1,641,740+
	-	1185	466,860
	-	1016	827,560
stress- relieved	733	847	42,440
	550	637	132,650
	550	637	183,250
	331	383	1,209,700+

+: runout

Table 3

Cyclically stable weld toe strains computed by finite element analysis
for stress-relieved specimens

Bending	Torsion	Strains, μ					
		ϵ_{xx}	ϵ_{yy}	ϵ_{zz}	γ_{xy}	γ_{yz}	γ_{xz}
N-m	N-M						
733	847	-390	-1572	1962	-300	-5771	3818
550	637	-45	-530	1371	-408	-1655	1231
331	383	-27	-320	825	-295	-1194	74

Table 4

Fatigue crack initiation life prediction for stress-relieved specimens

Bending N-m	Torsion N-m	N_f cycles	N_I , cycles (Predicted)		
			Maximum Shear Strain	Lohr-Ellison Parameter	Kandil-Brown Miller Parameter
773	847	42,440	1,033	1,863	1,538
550	637	132,650	55,850	60,500	77,000
550	637	183,250	55,850	60,500	77,000
331	383	1,209,700+	1,590,000	2,400,000	3,225,000

+: runout

Table 5

High cycle fatigue life predictions
made using the modified Basquin equation

Welds	Weld Toe Stresses		N_f Observed, cycles	N_f Predicted, cycles	
	S_a^B	τ_a^T		Equ. Stress	Max. Principal Stress
	MPa	MPa			
as-welded	216	-	198,000	32,791	32,791
"	193	-	145,000	114,663	114,663
"	172	-	560,850	409,671	409,671
"	159	-	624,330	1,045,475	1,045,475
"	159	92	220,030	211,979	360,113
"	130	75	788,370	2,042,793	3,467,552
"	130	75	1,641,740+	2,042,793	3,467,552
stress- relieved	130	75	132,650	51,433	87,302
"	130	75	183,650	51,433	87,302
"	78	45	1,209,700+	15,667,520	26,611,197

+: runout

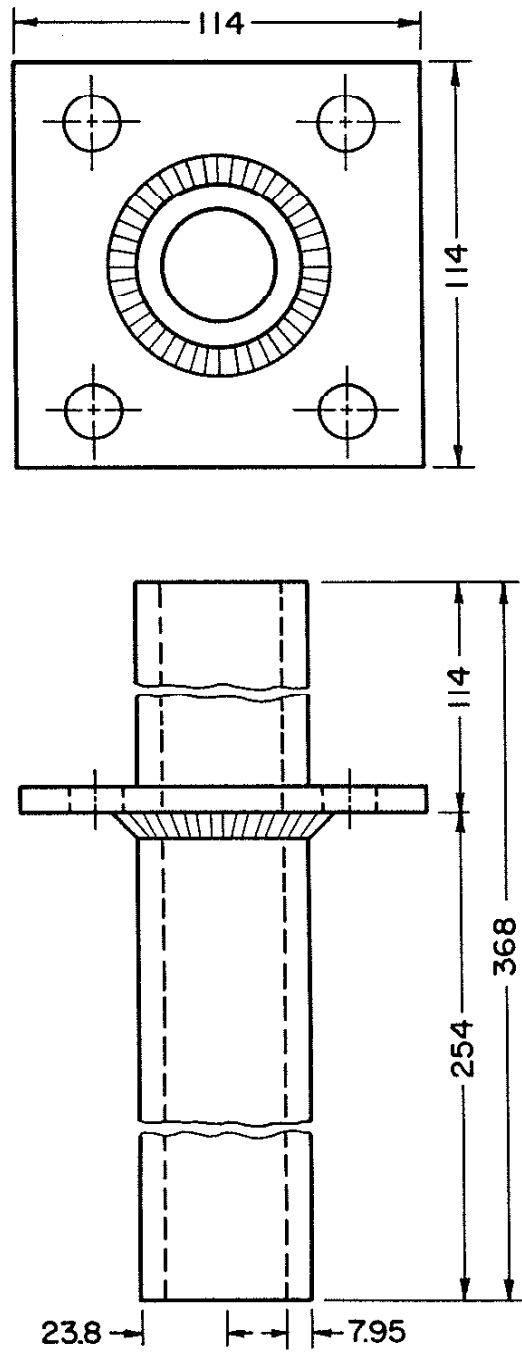


Fig. 1 Specimen geometry of tube-to-plate welds (units in mm).

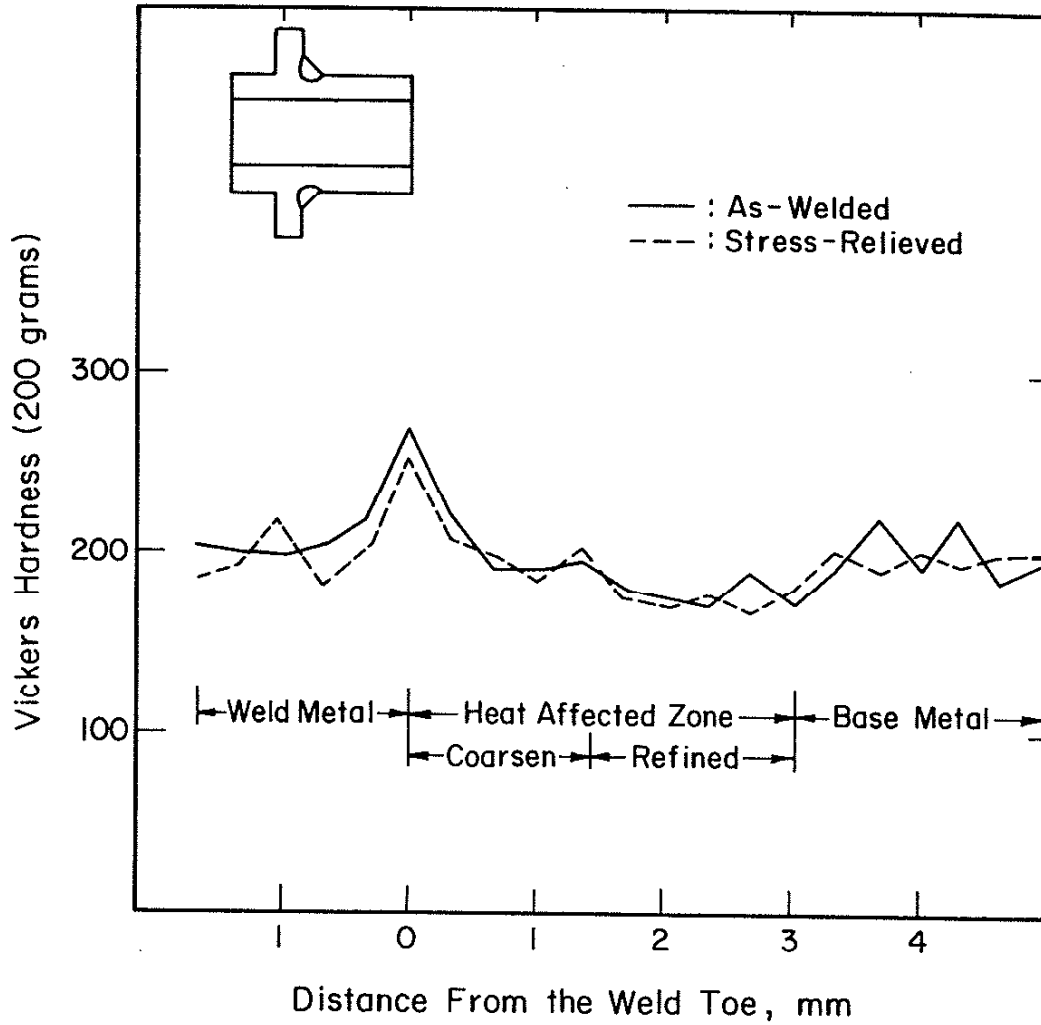


Fig. 2 Results of Vickers pyramid hardness (200 grams load) surveys 0.15 mm below the surface of steel tubing.

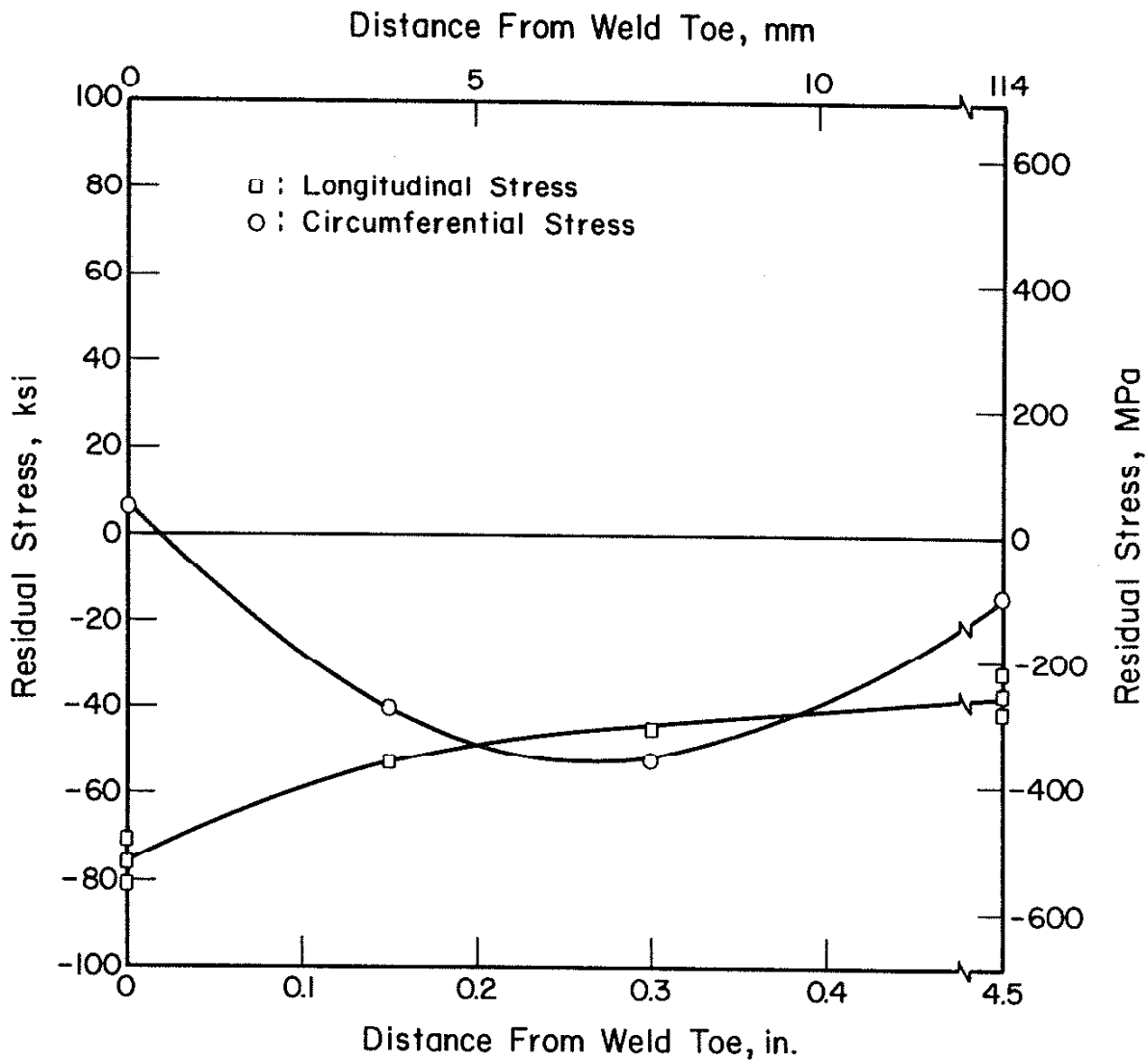


Fig. 3 Residual stress distribution on the outer surface of tube-to-plate specimen.

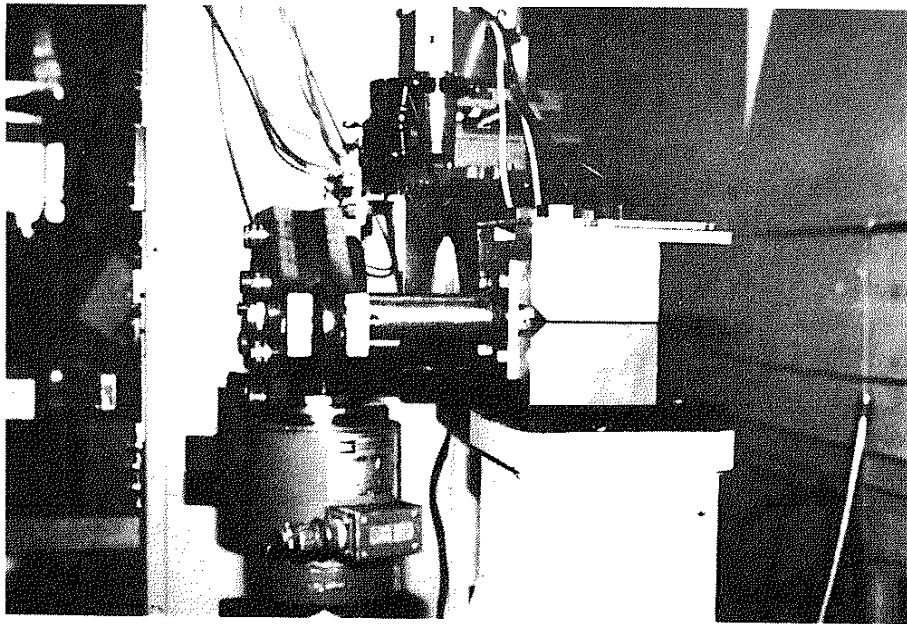


Fig. 4 Testing apparatus for welds subjected to combined bending and torsion

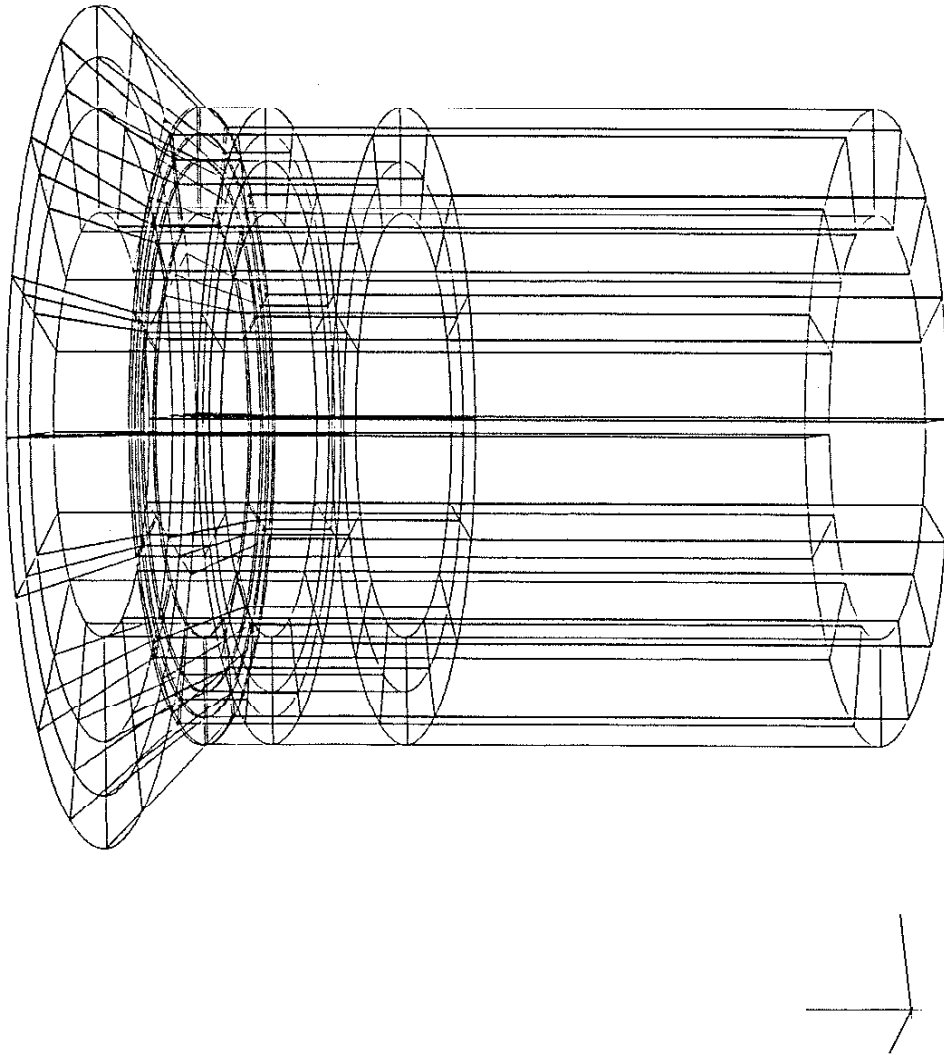


Fig. 5 Finite element mesh of tube-to-plate welds (ratio of notch-root element size to notch radius = 1:4).

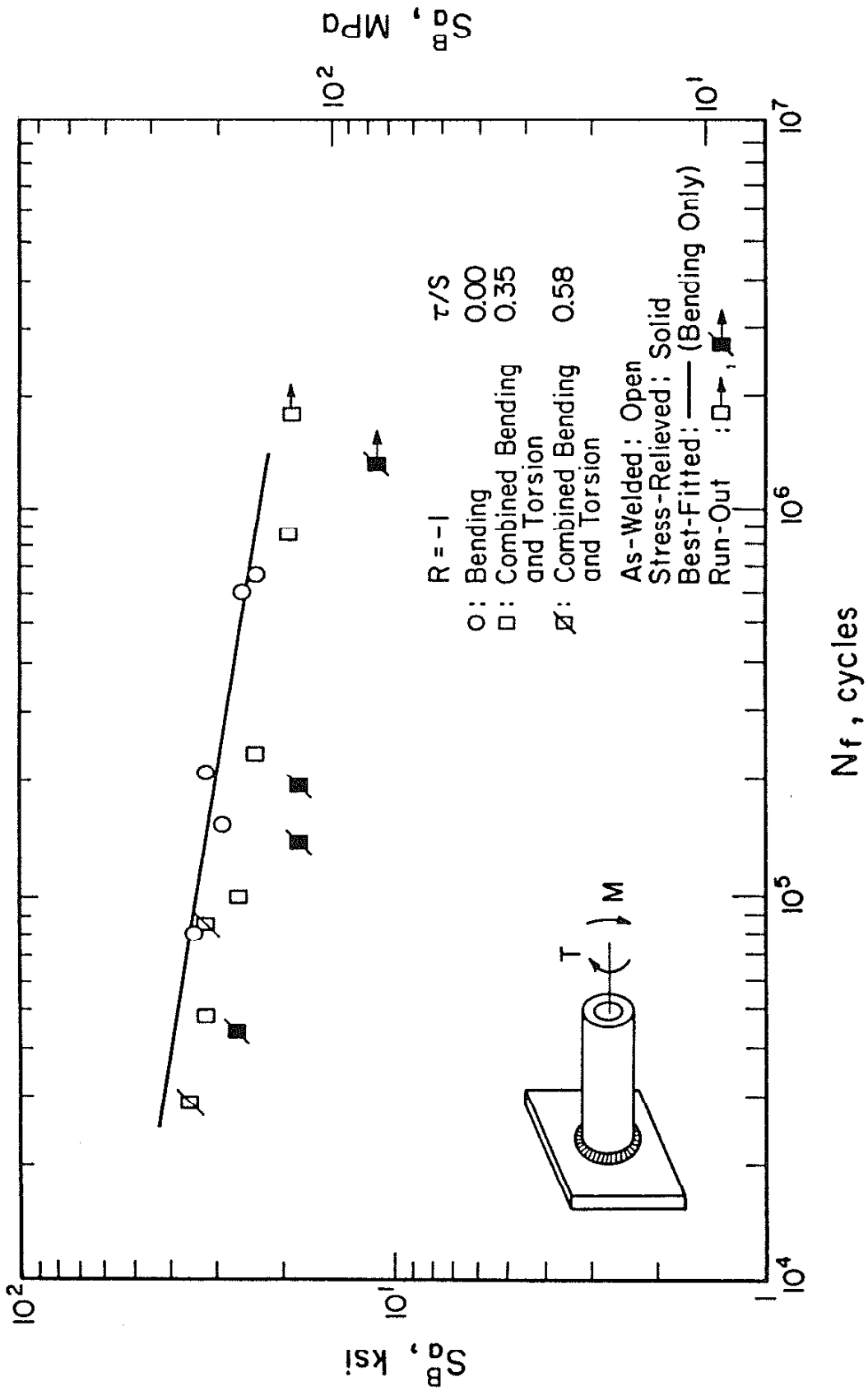


Fig. 6 Fatigue life versus bending stress amplitude for as-welded tube-to-plate specimens with a stress ratio $R = -1$.

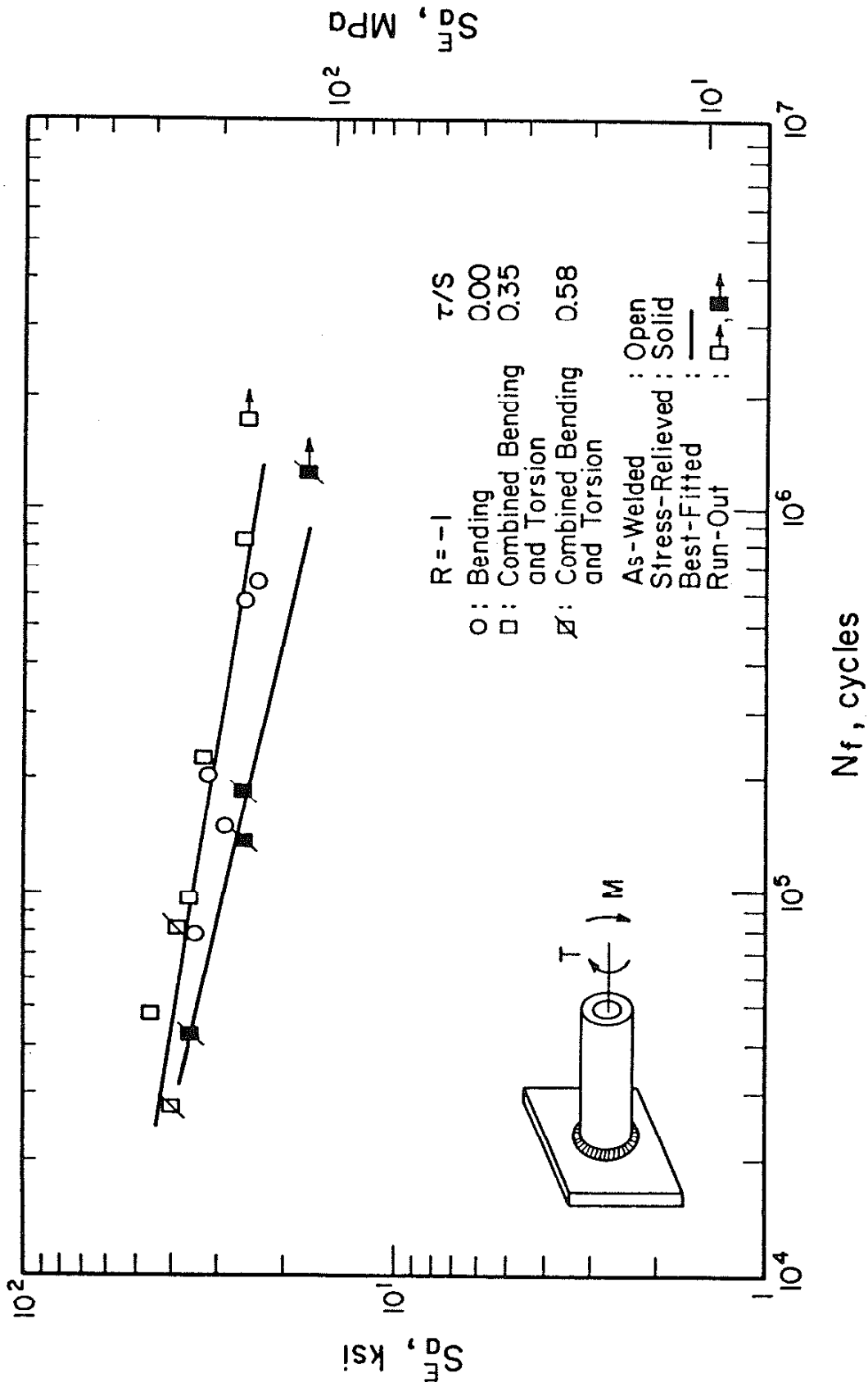


Fig. 7 Fatigue life versus equivalent stress amplitude (octahedral stress amplitude) for as-welded and stress-relieved tube-to-plate specimens with a stress ratio $R = -1$.

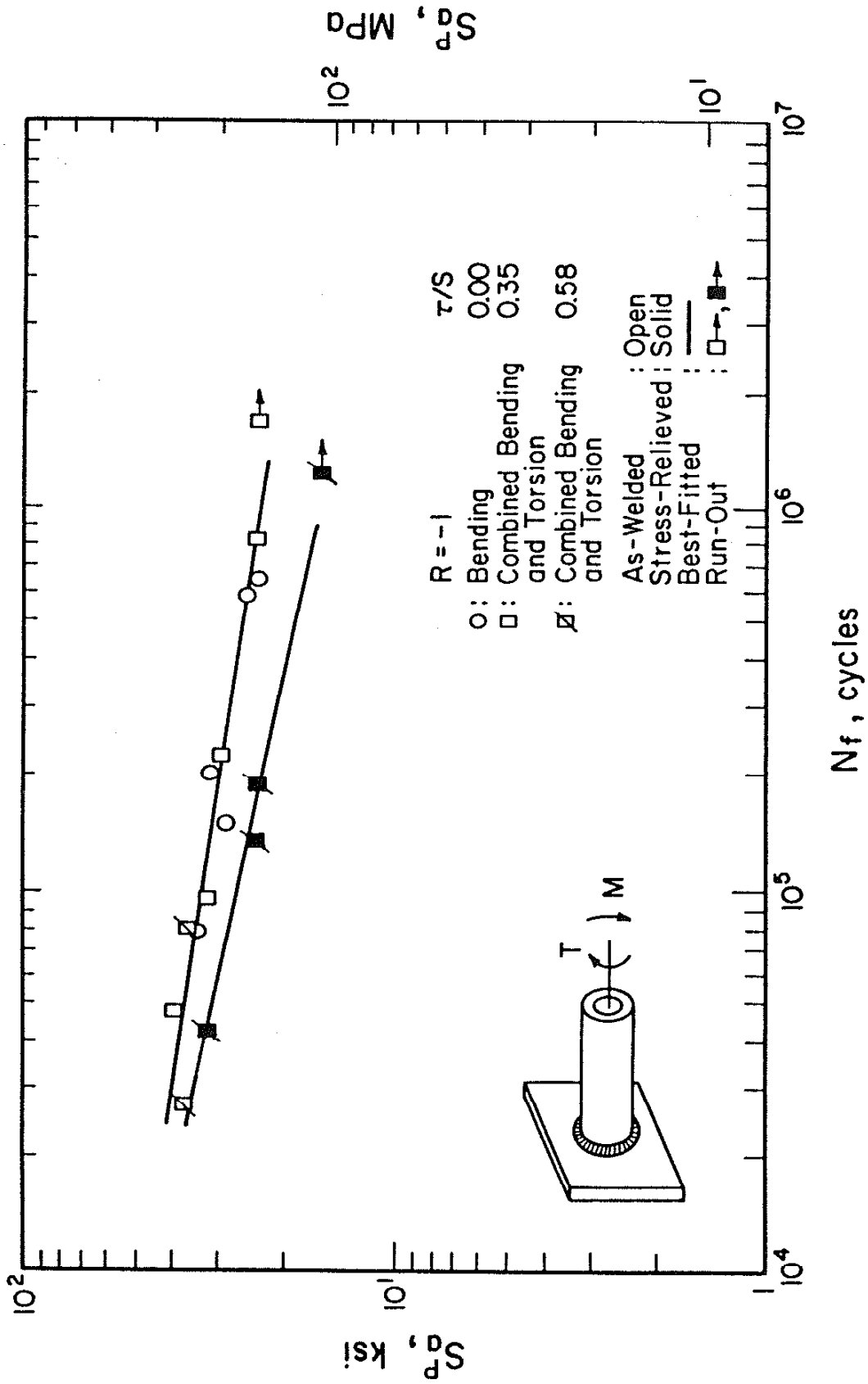


Fig. 8 Fatigue life versus maximum principal stress amplitude for as-welded and stress-relieved tube-to-plate specimens with a stress ratio $R = -1$.

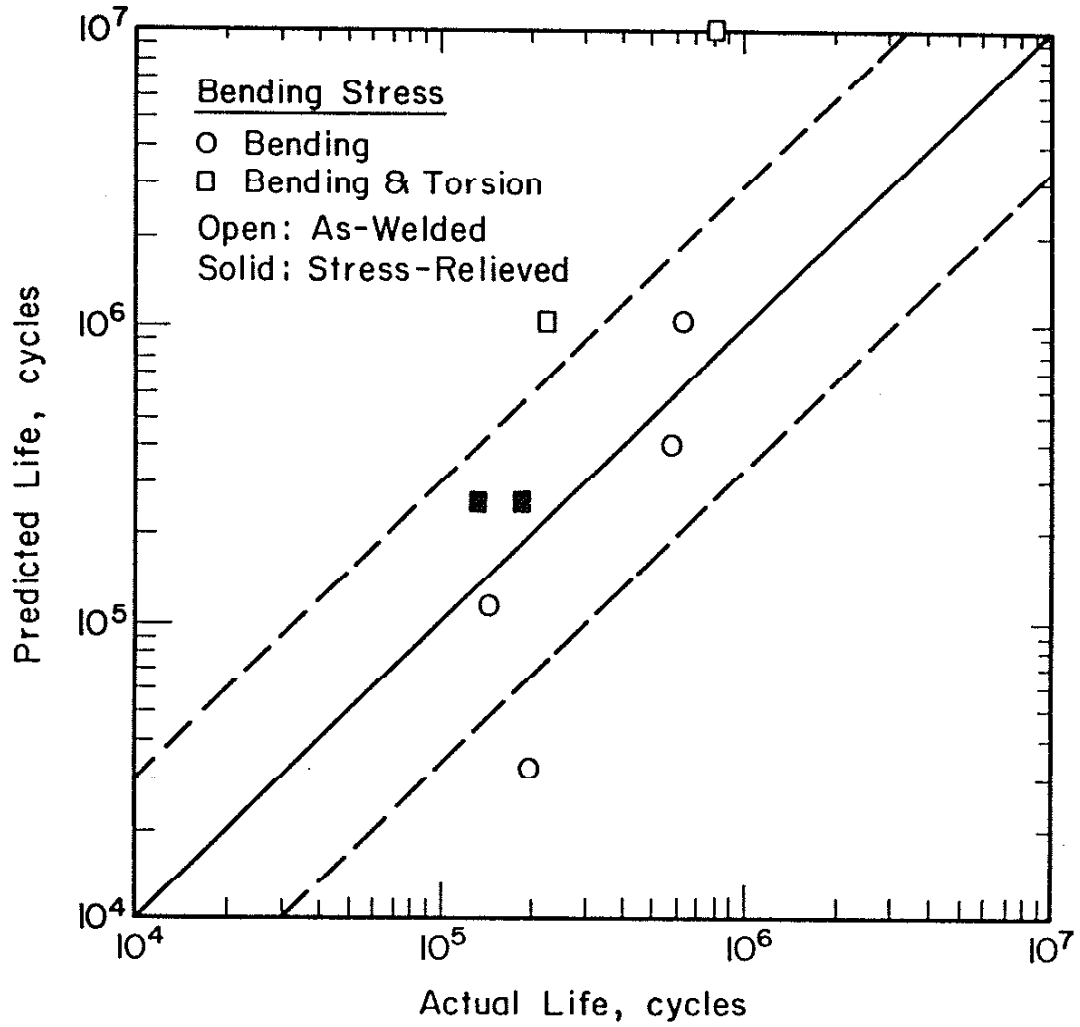


Fig. 9 Comparison of actual and predicted fatigue life using local bending stress and the modified Basquin equation.

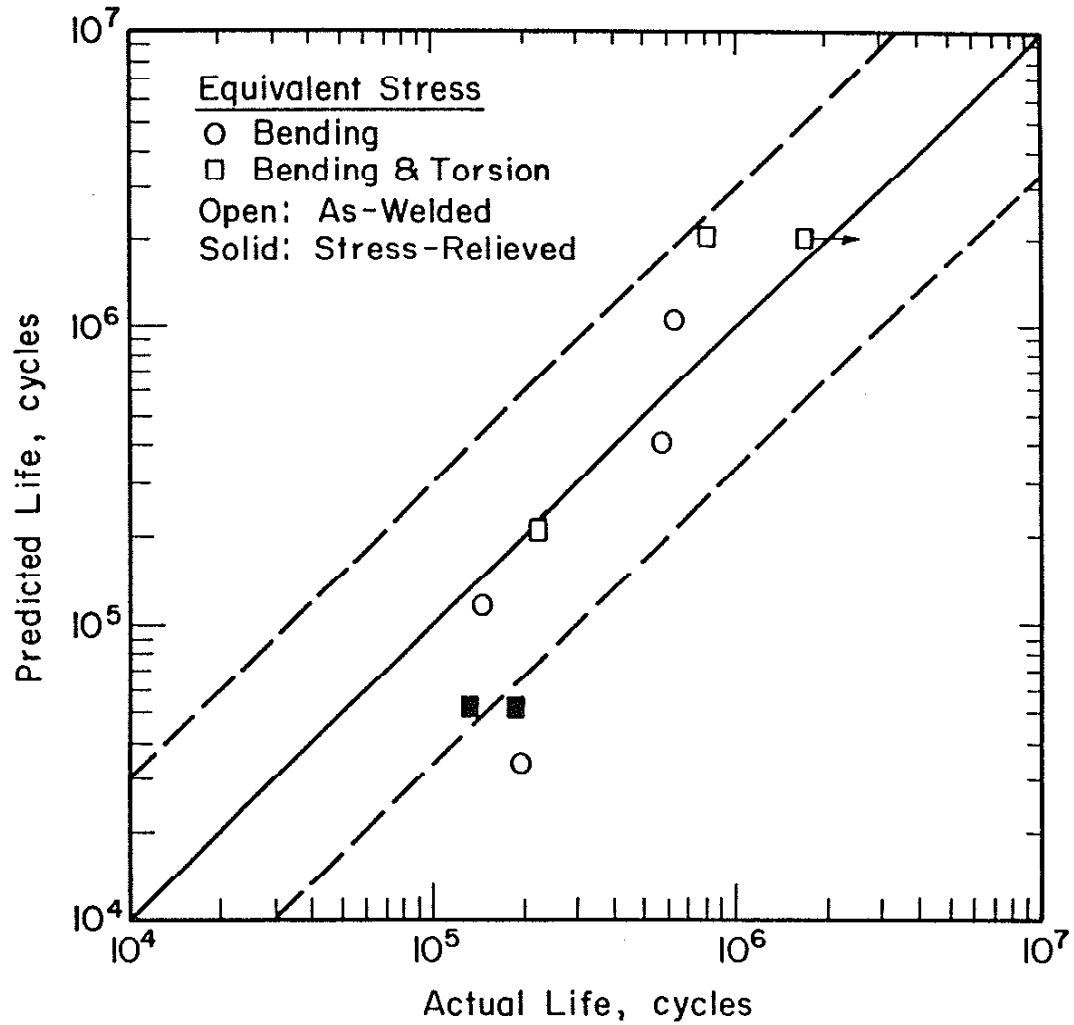


Fig. 10 Comparison of actual and predicted fatigue life using local equivalent stress amplitude (octahedral shearing stress amplitude) and the modified Basquin equation.